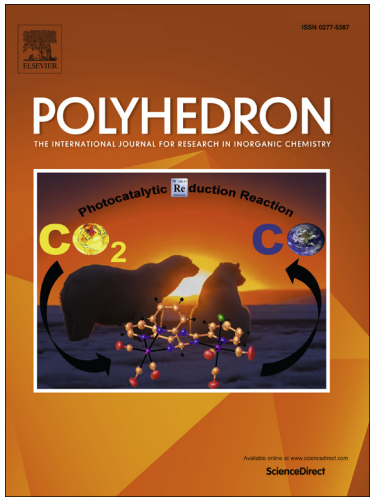

Synthesis, Characterization and DFT Study of a New Family of Pyrazole Derivatives

Rodrigo Faundez, Desmond Macleod-Carey, Ximena Zarate, Carlos Bustos, Elies Molins, Eduardo Schott

PII: S0277-5387(14)00402-1
DOI: http://dx.doi.org/10.1016/j.poly.2014.06.003
Reference: POLY 10800

To appear in: *Polyhedron*

Received Date: 17 April 2014
Accepted Date: 3 June 2014

Please cite this article as: R. Faundez, D. Macleod-Carey, X. Zarate, C. Bustos, E. Molins, E. Schott, Synthesis, Characterization and DFT Study of a New Family of Pyrazole Derivatives, *Polyhedron* (2014), doi: http://dx.doi.org/10.1016/j.poly.2014.06.003

Synthesis, Characterization and DFT Study of a New Family of Pyrazole Derivatives

Rodrigo Faundez[a,b], Desmond Macleod-Carey[c], Ximena Zarate[b], Carlos Bustos[d], Elies Molins[e] and Eduardo Schott[b*]

[a]*Departamento de Ciencias Quimicas, Universidad Católica de Chile, Avda. Vicuña Mackenna 4860, Macul, Chile.*

[b]*Laboratorio de Bionanotecnologia, Universidad Bernardo O'Higgins, General Gana 1702, Santiago, Chile.*

[c]*Universidad Autónoma de Chile, Inorganic Chemistry and Molecular Materials Group, Carlos Antúnez 1920, Santiago, Chile*

[d]*Instituto de Ciencias Quimicas, Universidad Austral de Chile, Avda. Los Robles sin numero, Valdivia, Chile.*

[e]*Institut de Ciencia de Materials de Barcelona (CSIC), Campus de la UAB, 08193 Cerdanyola, Barcelona, Spain*

*email:maschotte@gmail.com, Phone:+56-2-24772243

Abstract

This work deals about the synthesis and characterization of compounds containing the pyrazole core belonging to the family of (E)-4-((3,5-dimethyl-1-(4-R-phenyl)-1H-pyrazol-4-yl)diazenyl)benzonitrile, with possible application as ligands in inorganic chemistry. These compounds were obtained by reaction of a substituted arilhydrazine, R-C_6H_4-$NHNH_2$, R: 4-OCH_3, 4-CH_3, 4-F, 4-H, 4-Cl, 4-CF_3, 4-CN, 3-Cl, 3-NO_2, 2-Cl and perfluorophenylhydrazine, C_6F_5-NH_2NH; with a β-diketohydrazone precursor of formula $(CH_3CO)_2C$=N-NH-C_6H_4-4-CN. Analytical techniques (MP and EA) and spectroscopic methods as UV-Vis, IR, ^{1}H-NMR, ^{13}C-NMR were employed to characterize the prepared systems. One of the synthesized compounds yielded in ethanol single crystals suitable for X-Ray diffraction study. In order to model all the studied compounds and the Molecular Orbitals involved in the transitions, DFT and TDDFT calculations were performed. The non-variability of the bond distances suggests the robustness of the conjugated structure formed by the R-C_6H_4-pyrazole-N=N-benzonitrile rings, which is poorly affected by the change of the substituents over the phenyl ring.

Introduction

Azole heterocycles are interesting because of their occurrence in the nature and as framework of synthetic molecules. Most of those molecules show biological activity and wide application in all areas of coordination chemistry. In the field of coordination chemistry, pyrazoles have attracted considerable interest because their conjugate bases, pyrazolates, have been found to bind metals in a variety of modes and, in particular, are very strong bridging ligands.[1–3] For example, pyrazolato complexes have been used as starting material for chemical vapour deposition, furthermore they have interesting luminescent properties.[4–7] Most pyrazoles have biological (anti-neoplasic, anti-microbial, anti-inflammatory, anti-diabetic, in between others) and can also be used as ligands or as precursors of pyrazolate-based ligands and are accessible by well-established synthetic methods.[2-4,8] These methods are quite general, which allow the preparation of pyrazoles with a variety of substitution patterns and with different substituents in several positions of the pyrazole ring.[9–12] Moreover, pyrazole and pyrazolate rings can be included as part of polydentate ligands.[13–15] In this sense, polypyrazolylborates are the most useful and widely employed ligands in different areas of coordination chemistry.[16]

The conjugate acids (or protonated forms) of the pyrazoles, namely, the pyrazolium cations, are present in many salts. The behavior of pyrazolium cations as supramolecular guests toward certain hosts has been studied and it has been shown that pyrazolium cations play crucial roles in some cases.[17–19]

Complexes that contain one or more pyrazolato ligands can be prepared by reacting the preformed alkaline pyrazolate salts with suitable metal complexes (e.g., halide complexes, so that the pyrazolate anion replaces the halide), or by treating the preformed pyrazole complexes with a base.[20] However, the employment of preformed pyrazolate salts or pyrazole complexes is not required for the synthesis of metal pyrazolato complexes in many cases, whereas they can be directly formed from the suitable metal precursor, the pyrazole and a base.[21]

Furthermore, pyrazoles are able to fully accept or donate H^+. In this sense the basic site of the pyrazole molecule can act as a hydrogen-bond acceptor, whereas the N–H group can act as a hydrogen-bond donor. The ability of this N–H group to act as a hydrogen-bond donor is the main reason why pyrazoles are important molecules in supramolecular chemistry. The particular type of aggregation that occurs in the solid-state structure of N–H pyrazoles has been found to be largely dependent on the substitution pattern of the pyrazole ring.[22,23]

In a previous communication, preliminary results have been reported about the synthesis of a large library of pyrazoles.[24–27] In the herein review, an extensive report on the synthesis, characterization and theoretical studies of a series of (E)-4-((3,5-dimethyl-1-(4-**R**-phenyl)-1H-pyrazol-4-yl)diazenyl)benzonitrile, see Figure 1, was made (with **R**= 4-OCH_3 (**1**), 4- CH_3 (**2**), 4-H (**3**), 4-F (**4**), 4-Cl (**5**), 4-CF_3 (**6**), 4-CN (**7**), 3-Cl (**8**), 3-$N0_2$ (**9**), 2-Cl (**10**)) and perfluorophenylhydrazine (**11**)). Suitable crystals of **11** for X-Ray diffraction studies were obtained, in order to corroborate the proposed structure. Furthermore, DFT and TDDFT calculations were performed to determine the composition of the frontier molecular orbitals (FMO), to model the UV-Vis transition and to assign their character.

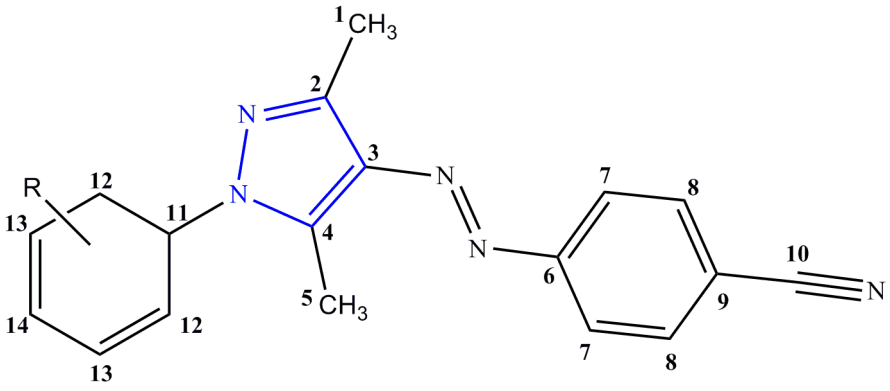

Figure 1. General structure of the studied pyrazoles and the corresponding numeration used for the NMR assignation. The pyrazole ring is shown in blue and R- are: 4-OCH_3 (**1**). 4-CH_3 (**2**), 4-H (**3**), 4-F (**4**), 4-Cl (**5**), 4-CF_3 (**6**), 4-CN (**7**), 3-Cl (**8**), 3-$N0_2$ (**9**), 2-Cl (**10**), and -C_6F_5 (**11**).

Experimental

Chemicals

Aniline, 4-aminobenzonitrile, acetylacetone, sodium nitrite, acetic acid, hydrochloric acid, sodium hydroxide and substituted hydrazine R-C_6H_4-$NHNH_2$ (R= 4-OCH_3 (**1**). 4- CH_3 (**2**), 4-H (**3**), 4-F (**4**), 4-Cl (**5**), 4-CF_3 (**6**), 4-CN (**7**), 3-Cl (**8**), 3-NO_2 (**9**), 2-Cl (**10**)) and perfluorophenylhydrazine (**11**) were purchased from Sigma-Aldrich. Besides, solvents: methanol, ethanol, diethyl ether, acetone $CDCl_3$ and DMSO-d_6, were purchased from usual commercial sources, like the Merck, Fisher and J.T. Baker providers. All the precursors and solvents were used without further purification. - diketohydrazone precursor, 4-(2-(2,4-dioxopentane-3-yliden)hydrazine)benzonitrile, was obtained as described in literature[27–29] and its structure was checked by IR spectroscopy.

Physical measurements

Uncorrected melting points, MP, were determined on digital STUARD, SMP10 apparatus. Elemental analysis, EA, was obtained from a FISONS, EA 1118 microanalyses using sulfanilamide as standard. UV-Vis spectra were recorded between 600 and 235 nm, in quartz cells with 1 cm length pass, using a Perking Elmer, Lambda 35 spectrophotometer. Concentrated solutions of each compound ($5.0x10^{-4}$ mol/L) were used and a dilution to $2.5x10^{-5}$ mol/L. The infra-red spectra, IR, were obtained in solid state on an ATR Jasco, PR0450-S, mounted on a Jasco, FT/IR-4200 equipment. Depending of the solubility of compounds, ^{1}H-NMR, ^{13}C-NMR and HMBC spectra were recorded by the standard methods in $CDCl_3$ or DMSO-d_6, using 5 mm i.d. glass tubes and the internal solvent signals as reference, in a Buker, Avance AM 400 spectrophotometer. Assignment of ^{1}H- and ^{13}C-NMR signals are reported using the numeration of Figure 1.

Data collection

Highly redundant single crystal X-Ray diffraction data set of **11** was collected at room temperature on a Bruker AXS SMART APEX CCD diffractometer using monochromatic MoKa radiation, λ=0.71069 Å and a 0,3° separation between frames. Crystal data, data collection and structure refinement parameters are shown in Table 1, while Table 2 contains the selected bond lengths and Figure 2 exhibits an ORTEP view of the molecule. Data integration was performed using SAINT program contained in the diffractometer software package. The structure was solved by using direct methods and Fourier's difference maps and refined by least squares on F^2 with anisotropic displacement parameters for non-H atoms. All hydrogen atoms are in calculated positions and were refined riding on their parent atoms. All performed calculations to solve the structure, to refine the model proposed and to obtain the results were carried out with the computer programs WinGX[30,31].

Table 1. Crystal data and data collection and refinement parameters of the X-ray crystal structure of compound **11**.

Empirical formula	$C_{18}H_{10}F_5N_5$
Weight formula	391.31
Temperature	294(2) K
Wavelength	0.71073 Å
Crystal system	Orthorhombic
Spatial group	*Fdd2*
Cell parameters	*a*= 19.335(7) Å, α= 90°
	b= 47.422(10) Å, β= 90°
	c = 7.545(3) Å, γ = 90°
Cell volume	6918(4) $Å^3$
Z	16
Calculated density	1.503 g/cc^3
Absorption coefficient	0.132 mm^{-1}

F(000)	3168
Crystal size	0.30 x 0.21 x 0.18 mm^3
Θ range for data collection	1.72 a 25.99°
Indices range	0≤ *h* ≤23, 0≤ *k* ≤58, -9≤ *l* ≤9
Reflections collected	7235
Independent reflections	3263 [*R(int)* = 0.0451]
Full value of θ=25.99°	99.9 %
Minimum and maximum transmission	0.9767 y 0.9616
Refinement method	Full-matrix least-squares on F^2
Data/ restraints/ parameters	3263/7/264
S (Goodness-of-fit on F^2)	0.838
Final R index with [$I > 2\sigma(I)$]	R_1 = 0.0485, wR_2 = 0.0765
R index all data	R_1 = 0.1748, wR_2 = 0.0998
Major difference peak/ hole	0.183 y -0.134 ē×Å^{-3}

Table 2. Calculated selected bond distances for the complete family of studied compounds and the experimental (exp.) report for compound **11**. All the data is in Å.

	1	**2**	**3**	**4**	**5**	**6**	**7**	**8**	**9**	**10**	**11**	**11_{exp}**
$N=N_{azo}$	1.265	1.265	1.265	1.264	1.264	1.264	1.263	1.264	1.263	1.264	1.263	1.188
$N\text{-}N_{pyr}$	1.377	1.377	1.377	1.377	1.377	1.378	1.378	1.377	1.378	1.378	1.379	1.372
$C_4\text{-}N_{pyr}$	1.375	1.376	1.376	1.377	1.377	1.378	1.379	1.377	1.379	1.377	1.379	1.446
$N_{pyr}\text{-}C_{11}$	1.414	1.415	1.415	1.423	1.415	1.415	1.415	1.415	1.415	1.415	1.416	1.567
$C_9\text{-}C_{10}$	1.429	1.429	1.429	1.429	1.429	1.429	1.429	1.429	1.429	1.429	1.429	1.420
$C_{10}\equiv N$	1.156	1.156	1.156	1.156	1.156	1.156	1.156	1.156	1.156	1.156	1.156	1.141
C-R	1.360	1.509	1.084	1.349	1.756	1.503	1.156	1.758	1.482	1.752	1.333	1.343
$N_{azo}\text{-}C_6$	1.424	1.424	1.424	1.415	1.421	1.420	1.417	1.421	1.418	1.423	1.411	1.408
$N_{pyr}=C_2$	1.317	1.317	1.316	1.317	1.316	1.316	1.315	1.316	1.316	1.317	1.316	1.320

General Procedure

In a 100 mL round-bottomed flask were added: 2,6x10^{-3} mol of the β-diketohydrazone 4-(2-(2,4-dioxo pentane-3-yliden)hydrazine)benzonitrile, 0.60g; 30 mL of ethanol, 5 mL of glacial acetic acid, and substituted hydrazine, R-C_6H_4-$NHNH_2$ (R= 4-OCH_3 **1**, 2,9x10^{-3} mol, 0,53 g; 4-CH_3 **2**, 3x10^{-3} mol, 0.50 g; 4-H **3**, 3.2x10^{-2} mol, 3.51 g; 4-F **4**, 3.1x10^{-3} mol, 0.50 g; 4-Cl **5**, 3.0x10-3, 0.53 g; 4-CF_3 **6**, 2.7x10-3 mol, 0.48 g; 4-CN **7**, 3.1x10-3 mol, 0.52 g; 3-Cl **8**, 3.0x10-3 mol, 0.53 g; 3-NO_2 **9**, 2.9x10^{-3} mol, 0.54 g; 2-Cl **10**, 3.0x10^{-3} mol, 0.53 g. and perfluorophenylhydrazine **11**, 2.6x10^{-3} mol, 0.51 g. The reaction mixture was heated at reflux temperature stirring magnetically during 18 h. For precipitation of each compound the mixture was cooled to -18ºC by 2 h and by addition of around 25 mL of water. The yellow-orange solids were filtered by suction, washed with abundant water and dried under vacuum at 40ºC by 24 h. All compounds were recrystallized from ethanol/H_2O mixtures of variable composition or pure ethanol, except compound **3** which was recrystallized from 1:1 THF/EtOH.

Analysis

Compound (1) *(E)-4-((1-(4-methoxyphenyl)-3,5-dimethyl-1H-pyrazol-4-yl)diazenyl)benzonitrile*. Yield: 65% Recryst. From EtOH. MP: 154ºC. EA: for $C_{19}H_{17}N_5O$ (Mι: 331,37 g/mol): Calc(%): C, 68.87; H, 5.17; N, 21.13; Found(%):C, 69.21; H, 5.28; N, 21.54. UV-Vis in THF 2.50 x 10^{-3} mole/L, λ_{max}, nm(logε): λ_1: 459sh λ_2: 358(4.51) λ_3: 243(4.35). IR, ν(cm^{-1}): ν(C-H, Ar): 3045w, 3032w; ν(C-H, Alif.): 2990w, 2977w, 2931w; ν(C≡N): 2222s; ν(C=N), ν(N=N) or ν(C=C): 1610w, 1591w, 1548m, 1520s, 1467m; ν(N-N): 1390s; ν(R): 2835w. ^{1}H-NMR (400 MHz, *DMSO-d_6*) δ(ppm): 7.99 (d, *J* = 8.6 Hz, 2H), 7.89 (d, *J* = 8.6 Hz, 2H), 7.57 – 7.44 (m, 2H), 7.19 – 6.98 (m, 2H), 3.83 (s, 3H), 2.59 (s, 3H), 2.47 (s, 3H). ^{13}C-NMR (*DMSO-d_6*) δ(ppm): 159.03, 155.21, 142.34, 141.20, 135.75, 133.64, 131.36, 126.20, 122.24, 118.69, 114.40, 111.45, 55.50, 14.01, 10.89.

Compound (2) *(E)-4-((3,5-dimethyl-1-p-tolyl-1H-pyrazol-4-yl)diazenyl)benzonitrile*. Yield: 60% Recryst. From EtOH/H_2O 9:1. MP: 200-201ºC. EA: for $C_{19}H_{17}N_5$ (Mι:315,37 g/mol): Calc(%): C, 72.36; H, 5.53; N, 22,21; Found(%):C, 73.16; H, 5.72; N, 22.27 UV-Vis in THF 2.50 x 10^{-3} mole/L, λ_{max}, nm(logε): λ_1: 456sh λ_2: 357(4.59) λ_3: 236(4.41). IR, ν(cm-1): ν (C-H, Ar.): 3050w, 3035w; ν(C-H, Alif.): 2987w,

2925w; ν(C≡N): 2221s; ν(C=N), ν(N=N) or ν(C=C): 1598w, 1548m, 1521s; ν(N-N): 1393s. ^{1}HNMR (400 MHz, *DMSO-d_6*), δ (ppm): 8.03 – 7.95 (m, 2H), 7.90 (d, *J* = 8.6 Hz, 2H), 7.49 (d, *J* = 8.3 Hz, 2H), 7.38 (d, *J* = 8.2 Hz, 2H), 2.63 (s, 3H), 2.49 (s, 3H), 2.40 (s, 3H). ^{13}C-NMR (*DMSO-d_6*) δ(ppm): 155.14, 142.44, 140.77, 137.78, 135.87, 135.79, 133.37, 129.51, 124.33, 122.04, 118.39, 111.36, 20.41, 13.63, 10.73

Compound (3) *(E)-4-(3,5-dimethyl-1-phenyl-1H-pyrazol-4-yl)diazenyl)benzonitrile*. Yield: 98% Recryst. From EtOH/THF. MP: 176-177 ºC. EA: for $C_{18}H_{15}N_5$ (Mι: 301,35 g/mol): Calc(%): C, 71.79; H, 5.02; N, 23.24; Found(%):C, 72.03; H, 5.13; N, 24.36. UV-Vis in THF 2.92 x 10^{-3} mole/L, λ_{max}, nm(logε): 450sh; 355 (4.71); 284sh. IR, ν(cm^{-1}): ν(C-H, Ar): 3087w, 3058w; ν(C-H, Alif.): 2990w, 2930w; ν(C≡N): 2221s; ν(C=N), ν(N=N) or ν(C=C): 1596w, 1551s, 1512s; ν(N-N): 1393s. ^{1}H-NMR (400 MHz, *DMSO-d_6*) δ(ppm): 8.00 (d, *J* = 8.6 Hz, 2H), 7.90 (d, *J* = 8.6 Hz, 2H), 7.61 (ddd, *J* = 15.3, 8.3, 4.8 Hz, 4H), 7.50 (dt, *J* = 9.2, 4.2 Hz, 1H), 2.65 (s, 3H), 2.48 (s, 3H). ^{13}C-NMR (*DMSO-d_6*) δ(ppm): 155.16, 142.58, 141.47, 138.40, 136.01, 133.65, 129.35, 128.35, 124.60, 122.29, 118.67, 111.57, 14.08, 10.99.

Compound (4) *(E)-4-((1-(4-fluorophenyl)-3,5-dimethyl-1H-pyrazol-4-yl)diazenyl)benzonitrile*. Yield: 86% Recryst. From EtOH. MP: 181-182ºC. EA: for $C_{18}H_{14}FN_5$ (Mι: 319.34 g/mol): Calc(%): C, 67.70; H, 4.42; N, 21.93; Found(%):C, 68.00; H, 4.64; N, 22.14. UV-Vis in EtOH 2.50 x 10^{-3} mole/L, λ_{max}, nm(logε): 456sh; 354 (4.72); 269sh. IR, ν(cm^{-1}): ν(C-H, ar): 3087w, 3067w, 3052w; ν(C-H, alif.): 2992w, 2971w, 2930w; ν(C≡N): 2221s; ν(C=N), ν(N=N) or ν(C=C): 1595s, 1552s, 1507s; ν(NN): 1396s. ^{1}H-NMR (400 MHz, *DMSO-d_6*) δ (ppm): 8.00 (d, *J* = 8.6 Hz, 2H), 7.90 (d, *J* = 8.6 Hz, 2H), 7.68 (m, *J* = 10.4, 5.2, 2.8 Hz, 2H), 7.47 – 7.37 (m, 2H), 2.63 (s, 3H), 2.48 (s, 3H). ^{13}C-NMR (*DMSO-d_6*) δ(ppm): 162.69, 160.25, 155.14, 142.60, 141.66, 136.28, 135.92, 134.84, 133.67, 127.02, 126.93, 122.30, 118.67, 116.34, 116.11, 111.61, 14.05, 10.86.

Compound (5) *(E)-4-((1-(4-chorophenyl)-3,5-dimethyl-1H-pyrazol-4-yl)diazenyl)benzonitrile*. Yield: 70% Recryst. From Toluene. MP: 215-216ºC. EA: for $C_{18}H_{14}ClN_5$ (Mι: 335.79 g/mol): Calc(%): C, 64.38; H, 4.20; N, 20.86; Found(%):C, 65.10; H, 4.35; N, 21.71. UV-Vis in Toluene 2.29 x 10^{-3} mole/L, λ_{max}, nm(logε): 445sh; 355 (4.46); 257sh. IR, ν(cm^{-1}): ν(C-H, ar): 3049w; ν(C-H,alif.): 2986w, 2968w, 2927w;

ν(C≡N): 2221s; ν(C=N), ν(N=N) or ν(C=C): 1595w, 1552s, 1507s; ν(N-N): 1393s. ^{1}HNMR (400 MHz, *DMSO-d_6*) δ(ppm): 7.99 (d, *J* = 8.5 Hz, 2H), 7.91 (d, *J* = 8.5 Hz, 2H), 7.71 – 7.57 (m, 4H), 2.67 (s, 3H), 2.50 (s, 3H). ^{13}C-NMR (*DMSO-d_6*) δ(ppm): 155.06, 142.82, 141.24, 137.14, 133.40, 132.60, 129.13, 126.10, 124.17, 122.10, 118.36, 111.53, 13.67, 10.72.

Compound (6) *(E)-4-(3,5-dimethyl-1-(4-(trifluoromethyl)phenyl)-1H-pyrazol-4-yl)diazenyl)benzonitrile*. Yield: 60% Recryst. From EtOH. MP: 144-145ºC. EA: for $C_{19}H_{14}F_3N_5$ (Mι: 369.34g/mol): Calc(%): C, 61.79; H, 3.82; N, 18.96; Found(%):C, 62.86; H, 3.87; N, 20.41. UV-Vis in EtOH 2.41 x 10-3 mole/L, λ_{max}, nm(logε): 446sh; 354 (4.89); 263sh. IR, ν(cm^{-1}): ν(C-H, Ar): 3085w, 3056w; ν(C-H, Alif.): 2998w, 2933w; ν(C≡N): 2228s; ν(C=N), ν(N=N) or ν(C=C): 1672w, 1616s, 1556m, 1525m; ν(N-N): 1396s. ^{1}H-NMR (400 MHz, *DMSO-d_6*) δ(ppm): 8.05-7.85 (m, 8H), 2.74 (s, 3H), 2.51 (s, 3H). ^{13}C-NMR (*DMSO-d_6*) δ (ppm): 154.98, 143.17, 142.99, 141.69, 141.50, 136.26, 133.40, 128.56 128.25, 127.93, 127.61, 126.36, 126.32, 126.28, 126.25, 124.66, 122.14, 118.33, 111.66, 13.75, 10.85.

Compound (7) *(E)-4-((1-(4-isocyanophenyl)-3,5-dimethyl-1H-pyrazol-4-yl)diazenyl)benzonitrile*. Yield: 91% Recryst. From EtOH. MP: 208-209ºC. EA: for $C_{19}H_{14}N_6$ (Mι: 323.35 g/mol): Calc(%): C, 69.25; H, 4.32; N, 25.75; Found(%):C, 69.75; H, 4.20; N, 25.88. UV-Vis in EtOH 2.73 x 10-3 mole/L, λ_{max}, nm(logε): 449sh; 353 (4.59); 261sh. IR, ν(cm^{-1}): ν(C-H, Ar): 3120w, 3065w; ν(C-H, Alif.): 2985w, 2936w; ν(C≡N): 2224s; ν(C=N), ν(N=N) or ν(C=C): 1602m, 1583w, 1552m, 1514s; ν(N-N): 1385s. ^{1}H-NMR (400 MHz, *DMSO-d_6*) δ(ppm): 8.03 (d, *J* = 7.9 Hz, 2H), 7.98 (d, *J* = 7.8 Hz, 2H), 8-10-7.80 (m, 4H), 2.74 (s, 3H), 2.50 (s, 3H). ^{13}C-NMR (*DMSO-d_6*) δ(ppm): 154.91, 143.36, 141.83, 141.77, 136.38, 133.37, 133.35, 124.47, 122.14, 118.30, 117.94, 111.70, 110.32, 13.79, 10.92.

Compound (8) *(E)-4-((1-(3-Chlorophenyl)-3,5-dimethyl-1H-pyrazol-4-yl)diazenyl)benzonitrile*. Yield: 75% Recryst. From EtOH. MP: 172ºC. EA: for $C_{18}H_{14}ClN_5$ (Mι: 335.79 g/mol): Calc(%): C, 64.38; H, 4.20; N, 20.86; Found(%):C, 65.03; H, 4.19; N, 21.05. UV-Vis in EtOH 2.50 x 10^{-3} mole/L, λ_{max}, nm(logε): 452sh; 353 (4.77); 257sh. IR, ν(cm^{-1}): ν(C-H, Ar): 3088w, 3066w; ν(C-H, Alif.): 2994w, 2932w, 2923w; ν(C≡N): 2220s; ν(C=N), ν(N=N) or ν(C=C): 1593s, 1585s, 1551s, 1504s; ν(N-N): 1391s. ^{1}H-NMR (400 MHz, *DMSO-d_6*) δ(ppm): 8.01 (d, *J* = 8.6 Hz, 2H), 7.92 (d, *J* = 8.6 Hz, 2H), 7.76 (d, *J* =

1.6 Hz, 1H), 7.67 – 7.55 (m, 3H), 2.70 (s, 3H), 2.49 (s, 3H). ^{13}C-NMR (*DMSO-d_6*) δ(ppm): 155.09, 142.87, 142.08, 139.64, 136.14, 133.69, 133.61, 131.01, 128.24, 124.33, 123.18, 122.35, 118.65, 111.72, 14.14, 10.93.

Compound (9) *(E)-4-(3,5-dimethyl-1-(3-nitrophenyl)-1H-pyrazol-4-yl)diazenyl)benzonitrile*. Yield: 90% Recryst. From EtOH/THF. MP: 188ºC. EA: for $C_{18}H_{14}N_5O_2$ (Mι: 346.34g/mol): Calc(%): C, 62.42; H, 4.07; N, 24.27; Found(%):C, 62.86; H, 4,06; N, 24.49. UV-Vis in EtOH/THF 2.51 x 10-3 mole/L, λ_{max}, nm(logε): 454sh; 351 (4.65); 255sh. IR, ν(cm^{-1}): ν(C-H, Ar): 3092w; ν(C-H, Alif.): 2990w, 2967w, 2923w; ν(C≡N): 2226s; ν(C=N), ν(N=N) or ν(C=C): 1617w, 1599w, 1557m, 1536s; ν(N-N): 1398s. ^{1}H-NMR (400 MHz, *DMSO-d_6*) δ(ppm): 8.61–7.32 (m, 8H), 2.75 (s, 3H), 2.52 (s, 3H). ^{13}C-NMR (*DMSO-d_6*) δ(ppm): 154.94, 148.14, 143.27, 141.90, 139.12, 136.20, 133.39, 130.69, 130.06, 122.43, 122.14, 118.79, 118.32, 111.69, 13.74, 10.77.

Compound (10) *(E)-4-((1-(2-Chlorophenyl)-3,5-dimethyl-1H-pyrazol-4-yl)diazenyl)benzonitrile*. Yield: 70% Recryst. From EtOH. MP: 154ºC. EA: for $C_{18}H_{14}ClN_5$ (Mι: 335.79 g/mol): Calc(%): C, 64.38; H, 4.20; N, 20.86; Found(%):C, 64.77; H, 4.21; N, 21.20. UV-Vis in EtOH 2.50 x 10^{-3} mole/L, λ_{max}, nm(logε): 435sh; 348(4.38); 240(4.03). IR, ν(cm^{-1}): ν(C-H, Ar.): 3093w, 3065w, 3046w; ν(C-H, Alif.): 2981w, 2964w, 2922w; ν(C≡N): 2226s; ν(C=N), ν(N=N) or ν(C=C): 1589w, 1579w, 1550s, 1505s; ν(N-N): 1395s. ^{1}H-NMR (400 MHz, *DMSO-d_6*) δ (ppm): 7.99 (d, *J* = 7.6 Hz, 2H), 7.91 (d, *J* = 7.7 Hz, 2H), 7.75 (d, *J* = 7.7 Hz, 1H), 7.61 (dt, *J* = 14.8, 7.0 Hz, 3H), 2.50 (s, 3H), 2.43 (s, 3H). ^{13}C-NMR (*DMSO-d_6*) δ (ppm): 155.08, 143.15, 141.74, 135.50, 135.13, 133.38, 131.40, 130.76, 130.08, 129.71, 128.23, 122.08, 118.36, 111.53, 13.45, 10.03.

Compound (11) *(E)-4-(3,5-dimethyl-1-(perfluorophenyl)-1H-pyrazol-4-yl)diazenyl)benzonitrile*. Yield: 85% Recryst. From EtOH. MP: 183ºC. EA: for $C_{18}H_{10}F_5N_5$ (Mι: 391.09: Calc(%): C, 55.25; H, 2.58; N, 17.90; Found(%): C, 55.74; H, 2.35; N, 18.52. UV-Vis in EtOH 2.50 x 10^{-3} mole/L, λ_{max}, nm(logε): 435sh; 340 (4.43); 239 (4.17). IR, ν(cm^{-1}): ν(C-H, Ar.): not found; ν(C-H, Alif.): 2931w; ν(C≡N): 2227s; ν(C=N), ν(N=N) or ν(C=C): 1602w, 1563w, 1536s, 1513s; ν(N-N): 1401s. ^{1}H-NMR (400 MHz, *DMSO-d_6*) δ

(ppm): 8.01 (d, J = 7.6 Hz, 2H), 7.93 (d, J = 7.8 Hz, 2H), 2.55 (s, 3H), 2.50 (s, 3H). ^{13}C-NMR (*DMSO-d_6*) δ (ppm): 154.85, 143.62, 136.28, 135.41, 133.44, 122.26, 112.02, 13.41, 9.46.

Computational Methods

The Gaussian 03 computational package[32] was used to perform ground-state geometry optimization calculations employing Becke's three-parameter hybrid exchange functional and the Lee–Yang–Parr non-local correlation functional B3LYP[33–35] and 6-31G* basis set was used for C, N, O, and H atoms and the LANL2DZ basis set[36,37] with an effective core potential for I.[38] Time-dependent density functional theory calculations were also performed using this methodology, and the first 60 singlet excited states were calculated. Calculations by the first-principles method were used to obtain accurate excitation energies and oscillator strengths. We modelled the solvent with the polarizable continuum model using Ethanol as the solvent.[39]

Results and Discussion

Structure and Geometrical Parameters

Figure 2 presents the crystal structure of **11**, while Table 1 provides a survey of crystallographic and refinement data; Table 2 shows some selected bond distances. The structure has been well refined with final indices, [I>2σ(l)], of R_1=0.0485 and wR_2=0.0765, Table 1. The relevant characteristics, Figure 2, are (i) the presence of the β-diketohydrazone bonded to a pyrazole core, confirming the route followed by the reaction, see proposed mechanism in the SI, and (ii) the planarity of the β-diketohydrazone bonded to the pyrazole core, see torsion angles in the SI.

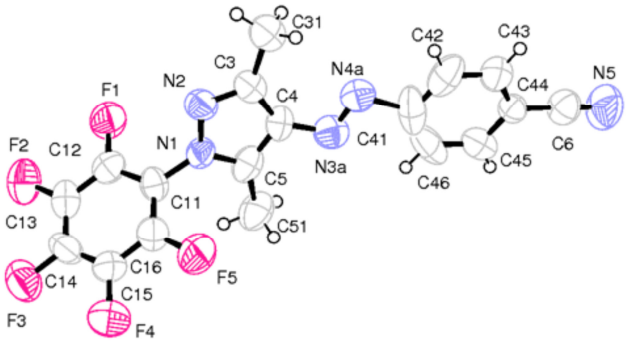

Figure 2. ORTEP representation of a molecule of compound **11** from its X-ray crystal structure showing the atom numbering and the displacement ellipsoids at 50% probability level (H atoms are drawn as circles of arbitrary radii).

By the DFT optimization of all the synthesized compounds we could make the comparison of the geometrical parameters as the substituents are changed over the phenyl ring bonded to the pyrazole core. The change of the substituents from an electron-donor substituent to another having an electron-acceptor character does not influence the calculated geometrical parameters of **1**-**11**. Also, as it is observed in Table 2, the calculated geometrical parameters are in good agreement with those obtained from the crystallographic study. This non-variability of the bond distances gives us a hint about the robustness of the conjugated structure formed by the phenyl-pyrazole-N=N-benzonitrile rings, which is poorly affected by the change of the -R substituents over the phenyl ring.

NMR spectroscopy

NMR assignments are made according to the numeration in Figure 1. A summary of the signals found in the ^{1}H-NMR spectra for **1**-**11** are shown in the supplementary information, see Table S1. According to Figure 1, the most important features of the ^{1}H-NMR spectra are the presence of: i) variable multiplicity resonances in the range 8.61-6.98 ppm, which correspond to the aromatic protons; ii) a singlet in the

range 2.75-2.50 ppm, which correspond to C^5-H protons of the methyl group CH_3-C=C; iii) a singlet located in the range 2.52-2.47 ppm, which corresponds to the protons 1C-H of the methyl group CH3-C=N and iv) **1** and **2** show the typical signals attributed to the methyl groups of the -R substituents (CH_3O- **1** and CH_3- **2**) located at 2.40 and 3.83 ppm, respectively.

The relative integration found for the signals H-Ar, ^{1}C-H, ^{5}C-H and H-R are 8:3:3:3 in **1** and **2**; 5:3:3 in **3**, 8:3:3 in **4**-**10** and 4:3:3 in **11**; which are consistent with the structure for each substituted pyrazole.

The signals found in the ^{13}C-NMR spectra are summarized in the supplementary information, see Table S2. Compounds **1**-**11** show the typical resonances C^1, C^2, C^3, C^4 and C^5, located at positions almost invariable, that are commonly found in the pyrazole ring. The signals associated to C^1, C^2, C^3, C^4 and C^5 are located in the ranges 11.26-9.46, 144.68-142.44, 137.14-131.73, 143.62-140.77 and 14.37-13.41 ppm, respectively. All the synthesized pyrazole show a signal in the range 112.02-111.36 ppm which is assigned to the C^{10} carbon of the nitrile group, C≡N. Besides, the non-fluorinated compounds show all the signals associated to the phenyl ring and to the corresponding substituent. However, compounds **4**, **6** and **11**, which are fluorinated, show split signals due to the C-F coupling. Detailed ^{13}C-NMR spectra of **4** and **6** are shown in the supplementary information. In compound **4** the C-F magnetic couplings of the carbons C^{14}, C^{12} and C^{13} are doublets located at 161.47 (d, J=245.7 Hz), 126.97 (d, J=8.9 Hz), 116.23 (d, J=23.1 Hz) ppm, respectively; C^{11} is a slightly deformed singlet located at 134.84 ppm. On the other hand, compound **6** shows no signal for C^{15}, C^{13} and C^{14} which should appear as quartets, while C^{11} and C^{12} are formally singlet, located at 134.01 and 118.74 ppm, respectively, see Figure S1. Finally, it was not possible to find the signals of the quaternary aromatic carbons in the perfluorophenyl group in **11**. This is due to the presence of couplings with more than one bond, which generates signals with high multiplicity that could not be distinguished from the background noise of the spectrum.

Optical Properties

Absorption bands found in the UV-vis spectra of **1**-**11** are collated in Table 3. The main characteristic of the spectra is determined by the general structure of the molecules. Each molecule has a double bond -N=N- (azo group) which is directly conjugated with one benzene rings and with the pyrazole ring. This fragment has an extensive electronic delocalization, therefore it is possible to predict the presence of a main absorption band associated to a π-delocalized system, that involves the fragment -N=N-, and other mainly associated internal transitions that emerge from the benzene rings and/or pyrazole system.

Table 3. Experimental (λ_{exp}) and calculated (λ_{Th}) wavelengths, logarithm of the extinction coefficient (logε), energy in eV (E), oscillator strength multiplied by 100 (*f*x100), active MOs and their percentage contributions for compounds **1**-**11** in THF.

Comp.	E	λ_{exp}	logε	λ_{Th}	*f*x100	% Orbtial Contribution			
1	2.603	459sh.		476	0.09	HOMO-1	→	LUMO	94
	3.579	359	4.51	346	65.36	HOMO-2	→	LUMO	94
	4.928	243	4.35	252	5.11	HOMO-6	→	LUMO	32
						HOMO	→	LUMO+1	46
2	2.601	456sh.		477	0.07	HOMO-1	→	LUMO	100
	3.184	357	4.59	389	107.76	HOMO	→	LUMO+1	100
	3.677	236	4.41	337	30.66	HOMO-2	→	LUMO+1	100
3	2.600	450sh.		477	0.10	HOMO-1	→	LUMO	100
	3.248	355	4.71	382	117.24	HOMO	→	LUMO	100
	4.492	284sh.		276	4.37	HOMO-6	→	LUMO	46
						HOMO	→	LUMO+1	50
4	2.601	456sh.		477	0.08	HOMO-1	→	LUMO	100
	3.238	354	4.72	383	112.88	HOMO	→	LUMO	100
	4.843	269sh.		256	1.33	HOMO	→	LUMO+1	26
						HOMO	→	LUMO+2	52
5	2.597	445sh.		477	0.04	HOMO-1	→	LUMO	100
	3.237	355	4.46	383	121.81	HOMO	→	LUMO	100
	4.843	257		256	4.03	HOMO-6	→	LUMO	63
						HOMO	→	LUMO+3	22
6	2.592	446sh.		478	0.01	HOMO-1	→	LUMO	100
	3.294	354	4.89	376	133.85	HOMO	→	LUMO	100
	4.494	263sh.		276	6.48	HOMO-5	→	LUMO	26

						HOMO-4	→	LUMO	22
						HOMO	→	LUMO+1	52
	2.586	449sh.		480	0.04	HOMO-1	→	LUMO	100
7	3.268	353	4.59	379	146.14	HOMO	→	LUMO	100
	4.689	261sh.		264	32.98	HOMO-2	→	LUMO+1	97
	2.595	452sh.		478		HOMO-1	→	LUMO	100
8	3.281	353	4.77	378	125.58	HOMO	→	LUMO	100
	4.784	257sh.		259	16.03	HOMO	→	LUMO+1	81
	2.593	454sh.		478	0.01	HOMO-1	→	LUMO+2	94
9	3.315	351	4.65	374	128.77	HOMO	→	LUMO+2	100
	4.751	255sh.		261	17.80	HOMO-5	→	LUMO+2	26
	2.611	435sh.		475	0.01	HOMO-1	→	LUMO	100
10	3.410	348	4.38	364	127.89	HOMO	→	LUMO	100
	5.155	240	4.03	241	10.98	HOMO	→	LUMO+3	67
	2.609	435sh.		475	0.01	HOMO-1	→	LUMO	100
11	3.444	340	4.43	360	131.48	HOMO	→	LUMO	100
	5.185	239	4.17	239	12.99	HOMO-2	→	LUMO+1	97

In this sense and in accordance with the structure of the compounds, we can determine that the first absorption band, λ_1, located in the range of 435-459 nm, of low intensity that appears as shoulder is attributed to a transition $\pi^*\leftarrow n$, that involves the azo bridge. While the second absorption band, λ_2, located in the range 340-357 nm, shows the highest extinction coefficient ($\log\varepsilon$=4.38-4.89) and is attributed to a transition $\pi^*\leftarrow\pi$. This transition involves the pyrazole and the benzonitrile rings. The remaining absorption band located at higher energy corresponds to λ_3 and is assigned of the type $\pi^*\leftarrow\pi$. Again, a similar behaviour of the previous transitions is observed.

All the former assignations were corroborated using TD-DFT calculation. An example of the involved MOs for compound **11** is presented in Figure 3. The image including all the studied compounds can be found in the supplementary information, Figure S2. In Table 3 are shown the experimental and calculated absorption maximum and the corresponding orbital contribution. As observed, λ_1 and λ_2 involve mainly

FMO, while λ_3 in some cases lower occupied and higher unoccupied MOs. The description of the FMO will be discussed in the DFT section.

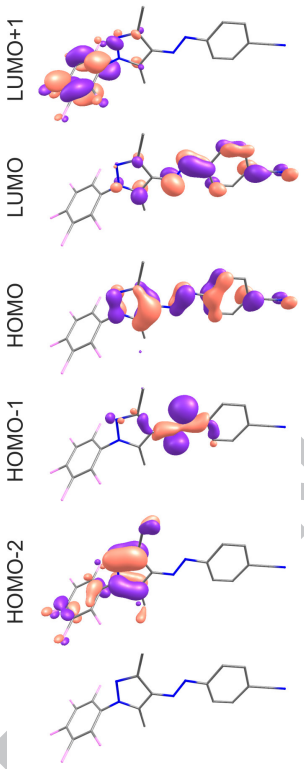

Figure 3. Diagram of the FMOs of compound **11**.

The main stretching absorptions found in the IR spectra of **1**-**11** are summarized as follows. In general, the spectra show a stretching ν(C-H) of aromatic protons, about 3000 cm^{-1} except **11** where no stretching of these protons were observed, which is due to the presence of the fluorinated substituent. This behaviour was corroborated with the DFT calculations. In all compounds, immediately under 3000 cm^{-1} a weak stretching ν(C-H) is observed. This stretching correspond to the aliphatic 3,5-dimethylpyrazole system. In case of compounds **1** and **2**, this signal includes stretching of the methyl groups present in the aromatic ring. Furthermore, it is possible to identify in the region 2228-2220 cm^{-1} in all compounds an intense band which corresponds to the stretching ν(C≡N) [40,41]. Additionally, there is a set of variable intensity bands

in the region 1672-1501 cm^{-1} attributed to the stretching ν(C=N), ν(N=N) and ν(C=C) [10,41–44]. It is also important to mention the signals attributed to the -R substituent of the benzene rings of compounds **1** ν(C-H), **6** ν(C-F) and **11** ν(C-F), located at 2835, 1183, 1116 and 1402 cm^{-1} respectively. Finally, all compounds show a stretching located between 1390 and 1401 cm^{-1} which is attributed to the N-N bond of the pyrazole ring.

DFT Calculations

The FMO are involved in almost every calculated transitions, *vide supra*. The FMO of all compounds show similar characteristics as observed in the supplementary information, see Figure S2. In all cases, the HOMO is delocalized over the pyrazole ring, the azo group and the benzonitrile ring. The HOMO-1 is composed in every case mainly by the azo bridge. In terms of the unoccupied MOs the LUMO is mainly centred over the benzonitrile ring. On the other hand, the LUMO+1 is located almost in every case over the substituted phenyl ring.

The HOMO, LUMO and GAP energies do not follow any trend. However all the calculated values are very similar and do not depend on the character of the substituent located over the phenyl substituent.

In order to make the first approach of the reactivity that this compounds might show, the estimated reactivity indexes (electronic chemical potential (μ), chemical hardness (η), and electrophilicity (ω))[45,46] are reported in Table 4.

Table 4. HOMO and LUMO orbital energies, HOMO-LUMO GAP and Reactivity indexes, electronic chemical potential (μ), chemical hardness (η) and electrophilicity (ω), all in eV.

Comp.	HOMO	LUMO	GAP	μ	η	ω
1	-6.11	-2.70	3.41	-4.40	1.71	5.68
2	-6.29	-2.71	3.57	-4.50	1.79	5.66
3	-6.36	-2.73	3.63	-4.54	1.81	5.68

4	-6.36	-2.74	3.62	-4.55	1.81	5.72
5	-6.39	-2.77	3.63	-4.58	1.81	5.78
6	-6.48	-2.80	3.68	-4.64	1.84	5.85
7	-6.51	-2.86	3.65	-4.69	1.82	6.02
8	-6.44	-2.77	3.66	-4.60	1.83	5.79
9	-6.51	-2.91	3.60	-4.71	1.80	6.16
10	-6.48	-2.72	3.77	-4.60	1.88	5.61
11	-6.60	-2.80	3.80	-4.70	1.90	5.81

η is a measure of the resistance of a chemical species to change its electronic configuration[45]. It is thought as an indicator, together with electronegativity, of the chemical reactivity and stability of systems. The highest value for η is shown by **11**, which has the perfluorinated substituent and is the most electron-attracting substituent. On the other hand the smallest value is shown by **1** which has the most electron-donor substituent. μ characterizes the tendency of escaping of electrons from the equilibrium system[45,46]; it is then related to the electronic charge rearrangement associated to any chemical process. This index shows an opposite behaviour to that of η, where the highest value is shown by **1**, which has the most electron donor substituent, and the smallest value is shown by **9** and **11** which have the most electron-acceptor substituents. Electrophilicity index, ω, could give information comparing two molecules in which one is an electrophile (or nucleophile) and this is indicated by a higher (or lower) ω[46]. In this case the highest value of ω was found for compound **9**, which has the most electron-attracting substituent. Comparing compounds with the substituent in position 4-, the highest value was found for compound **7**, which has the most electron-attracting substituent. On the other hand the smallest value of co was found for compound **10**. In case of comparing position 4-, the smallest value for ω was found for compound **1**, which has the most electron-donor substituent.

Conclusion

The high yield synthesis of a new family of pyrazoles of the type (E)-4-((3,5-dimethyl-1-(4-R-phenyl)-1H-pyrazol-4-yl)diazenyl)benzonitrile is reported. This procedure was performed by reaction of a b-

diketohydrazone 4-(2-(2,4-dioxopentane-3-yliden)hydrazine)benzonitrile with an arylhydrazine substituted, R-C_6H_4-$NHNH_2$, R=4-OCH_3 **1**; 4-CH_3 **2**; 4-F, **3**; 4-H, **4**; 4-Cl, **5**; 4-CF_3, 6; 4-CN, **7**; 3-Cl, **8**; 3-NO_2, **9**; 2-Cl, **10**; and pentafluorophenylhydrazine, NH_2NH-C_6F_5, **11**. This reaction has shown that the condensation of the b-diketohydrazone with arylhydrazine, occurs via a ketodihydrazone intermediary, which maintained under reflux for 36 h, undergoes an addition reaction with H_2O displacement to give the corresponding pyrazoles. Compounds **1**-**11** were purified by recrystallization and characterized by analytical and spectroscopic techniques (UV-Vis, IR and NMR). The crystal and molecular structure of the compound **11** was determined by single crystal X-ray diffraction. This structure shows a certain degree of positional disorder for the nitrogen atoms in the fragment –CN=NC-, which may be related with a vibrational coupled mode of this group. In any case, the fragment has nearly planar geometry (torsion angle τ(N3Aa- N4Aa- C41 - C42) = 169.6(6)º and τ(N4Aa - N3Aa- C4 - C3) = 0.4(11)º), which can be related with the extensive electronic delocalization, probably including adjacent rings to the pyrazole ring. All compounds were modelled by DFT calculations, showing similar geometrical parameters, which is adduced to the robustness of the conjugated system. Furthermore, TDDFT calculations were performed showing similar composition of the absorption bands in all the studied compounds.

Acknowledgment

ESV thanks FONDECYT 1130707. CBF thanks FONDECYT 1080269. EMG thanks EULANETCERMAT (PIRSES-GA-2011-295197).

Supplementary Information: The C-F coupling, full MO diagram, UV-Vis spectra, ^{1}H-NMR, ^{13}C-NMR and a summary of the crystallographic results can be found in the supplementary information. CCDC 983729 for **11** contains the full supplementary crystallographic data for this paper. These data can be obtained free of charge from The Cambridge Crystallographic Data Centre via www.ccdc.cam.ac.uk/data_request/cif.

References

[1] G. La Monica, G.A. Ardizzoia, in:, Prog. Inorg. Chem. Vol. 46, 1997, pp. 151–238.

[2] F. Meyer, Eur. J. Inorg. Chem. 2006 (2006) 3789.

[3] M. a Halcrow, Dalton Trans. (2009) 2059.

[4] A. a Mohamed, A. Burini, J.P. Fackler, J. Am. Chem. Soc. 127 (2005) 5012.

[5] M. a Omary, M. a Rawashdeh-Omary, M.W.A. Gonser, O. Elbjeirami, T. Grimes, T.R. Cundari, H.V.K. Diyabalanage, C.S.P. Gamage, H.V.R. Dias, Inorg. Chem. 44 (2005) 8200.

[6] H.V.R. Dias, H.V.K. Diyabalanage, M.G. Eldabaja, O. Elbjeirami, M. a Rawashdeh-Omary, M. a Omary, J. Am. Chem. Soc. 127 (2005) 7489.

[7] B. Hu, G. Gahungu, J. Zhang, J. Phys. Chem. A 111 (2007) 4965.

[8] R. Goikhman, T.L. Jacques, D. Sames, J. Am. Chem. Soc. 131 (2009) 3042.

[9] D. a. Mac-Leod-Carey, C. Bustos, E. Schott, L. Alvarez-Thon, M. Fuentealba, Acta Crystallogr. Sect. E Struct. Reports Online 63 (2007) m670.

[10] B. Yang, Y. Lu, C.-J. Chen, J.-P. Cui, M.-S. Cai, Dye. Pigment. 83 (2009) 144.

[11] R.D. Miller, O. Reiser, J. Heterocycl. Chem. 30 (1993) 755.

[12] K. Makino, H.S. Kim, Y. Kurasawa, J. Heterocycl. Chem. 35 (1998) 489.

[13] R. Mukherjee, Coord. Chem. Rev. 203 (2000) 151.

[14] A. Otero, J. Fernández-Baeza, A. Lara-Sánchez, J. Tejeda, L.F. Sánchez-Barba, Eur. J. Inorg. Chem. 2008 (2008) 5309.

[15] J. Klingele, S. Dechert, F. Meyer, Coord. Chem. Rev. 253 (2009) 2698.

[16] S. Trofimenko, Polyhedron 23 (2004) 197.

[17] S. Kiviniemi, A. Sillanp, M. Nissinen, K. Rissanen, M.T. Lämsä, J. Pursiainen, Chem. Commun. (1999) 897.

[18] S. Kiviniemi, M. Nissinen, M.T. Lämsä, J. Jalonen, K. Rissanen, J. Pursiainen, New J. Chem. 2000 (2000) 47.

[19] S. Kiviniemi, M. Nissinen, T. Alaviuhkola, K. Rissanen, J. Pursiainen, J. Chem. Soc. Perkin Trans. 2 6 (2001) 2364.

[20] G.A. Ardizzoia, G. LaMonica, A. Maspero, M. Moret, N. Masciocchi, Eur. J. Inorg. Chem. 1998 (1998) 1503.

[21] L.R. Falvello, J. Fornie, A. Martín, V. Sicilia, P. Villarroya, Organometallics 21 (2002) 4604.

[22] K. Umakoshi, Y. Yamauchi, K. Nakamiya, T. Kojima, M. Yamasaki, H. Kawano, M. Onishi, Inorg. Chem. 42 (2003) 3907.

[23] J. Pérez, L. Riera, Eur. J. Inorg. Chem. 2009 (2009) 4913.

[24] C. Bustos, C. Sanchez, R. Martinez, R. Ugarte, E. Schott, D. Macleodcarey, M. Garland, L. Espinoza, Dye. Pigment. 74 (2007) 615.

[25] C. Bustos, E. Schott, D. a. Mac-Leod-Carey, A. Ibañez, L. Alvarez-Thon, Acta Crystallogr. Sect. E Struct. Reports Online 62 (2006) o2499.

[26] C. Bustos, E. Schott, M. Ríos, C. Sánchez, J.-G. Cárcamo, J. Chil. Chem. Soc. 54 (2009) 267.

[27] C. Bustos, M. Pérez-Cerda, L. Alvarez-Thon, E. Barrales-Salcedo, M.T. Garland, Acta Crystallogr. Sect. E Struct. Reports Online E68 (2012) o353.

[28] V. Bertolasi, P. Gilli, V. Ferretti, K. Vaughan, New J. Chem. 23 (1999) 1261.

[29] H.C. Yao, J. Am. Chem. Soc. 29 (1964) 2959.

[30] G.M. Sheldrick, Acta Crystallogr. Sect. A Found. Crystallogr. 46 (1990) 467.

[31] L.J. Farrugia, J. Appl. Crystallogr. 32 (1999) 837.

[32] M.A.R. M.J. Frisch, G.W. Trucks, H.B. Schlegel, P.M.W. Gill, B.G. Johnson, M.A. J.R. Cheeseman, T.A. Keith, G.A. Petersson, J.A. Montgomery, K. Raghavachari, B.B.S. Al-Laham, V.G. Zakrzewski, J.V. Ortiz, J.B. Foresman, J. Cioslowski, J.L. A. Nanayakkara, M. Challacombe, C.Y. Peng, P.Y. Ayala, W. Chen, M.W. Wong, D.J.D. Andres, E.S. Replogle, R. Gomperts, R.L. Martin, D.J. Fox, J.S. Binkley, J.A.P. J. Baker, J.P. Stewart, M. Head-Gordon, C. Gonzalez, (n.d.).

[33] A.D. Becke, Phys. Rev. A 38 (1988) 3098.

[34] C. Lee, W. Yang, R.G. Parr, Phys. Rev. B 37 (1988) 785.

[35] A.D. Becke, J. Chem. Phys. 98 (1993) 5648.

[36] P.J. Hay, W.R. Wadt, J. Chem. Phys. 82 (1985) 270.

[37] W.R. Wadt, P.J. Hay, J. Chem. Phys. 82 (1985) 284.

[38] V.A. Rassolov, M.A. Ratner, J.A. Pople, P.C. Redfern, L.A. Curtiss, J. Comput. Chem. 22 (2001) 976.

[39] M. Cossi, G. Scalmani, N. Rega, V. Barone, J. Chem. Phys. 117 (2002) 43.

[40] M. Onishi, M. Yamaguchi, S. Kumagae, H. Kawano, Y. Arikawa, Inorganica Chim. Acta 359 (2006) 990.

[41] T.E. Ali, Heteroat. Chem. 24 (2013) 426.

[42] M.J. Ahsan, H. Khalilullah, S. Yasmin, S.S. Jadav, J. Govindasamy, Biomed Res. Int. 2013 (2013).

[43] B. Chandrakantha, A.M. Isloor, K. Sridharan, R. Philip, P. Shetty, M. Padaki, Arab. J. Chem. 6 (2013) 97.

[44] M. Asniza, A.M. Issam, H.P.S.A. Khalil, Sains Malaysiana 40 (2011) 765.

[45] R.G. Pearson, J. Mol. Struct. THEOCHEM 255 (1992) 261.

[46] P.K. Chattaraj, S. Giri, Annu. Rep. Prog. Chem.{,} Sect. C Phys. Chem. 105 (2009) 13.

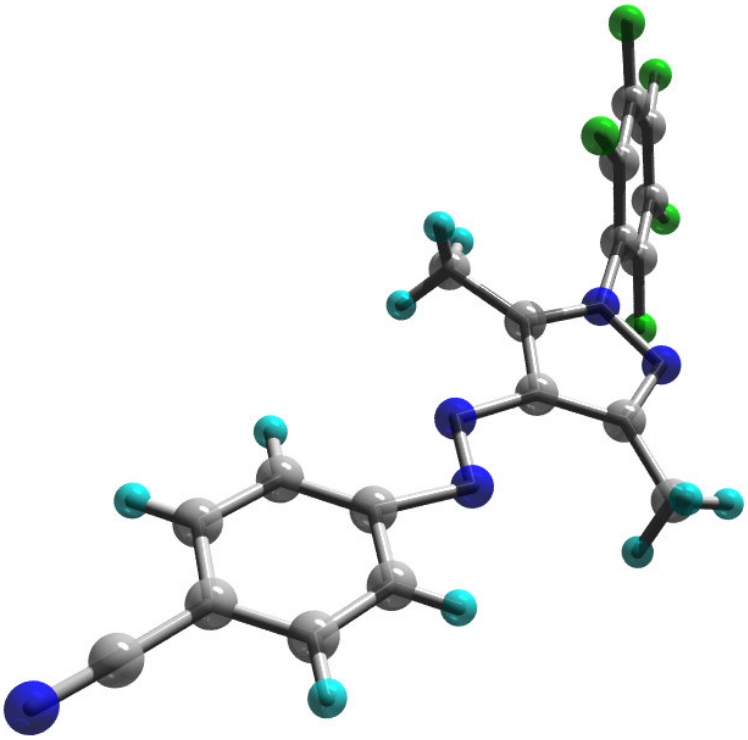

Synthesis and characterization of compounds containing the pyrazole nuclei